# Combined inverse-forward artificial neural networks for fast and accurate estimation of the diffusion coefficients of cartilage based on multi-physics models

Arbabi, Vahid; Pouran, Behdad; Weinans, Harrie; Zadpoor, Amir

**DOI**
10.1016/j.jbiomech.2016.06.019

**Publication date**
2016

**Document Version**
Proof

**Published in**
Journal of Biomechanics


www.elsevier.com/locate/jbiomech

# Combined inverse-forward artificial neural networks for fast and accurate estimation of the diffusion coefficients of cartilage based on multi-physics models

Vahid Arbabi, Behdad Pouran, Harrie Weinans, Amir A. Zadpoor

PII: S0021-9290(16)30693-5
DOI: http://dx.doi.org/10.1016/j.jbiomech.2016.06.019
Reference: BM7773

To appear in: *Journal of Biomechanics*

Received date: 13 January 2016
Revised date: 11 June 2016
Accepted date: 18 June 2016

Cite this article as: Vahid Arbabi, Behdad Pouran, Harrie Weinans and Amir A. Zadpoor, Combined inverse-forward artificial neural networks for fast and accurate estimation of the diffusion coefficients of cartilage based on multi physics models, *Journal of Biomechanics* http://dx.doi.org/10.1016/j.jbiomech.2016.06.019

*Original article*

# Combined inverse-forward artificial neural networks for fast and accurate estimation of the diffusion coefficients of cartilage based on multi-physics models

Vahid Arbabi[1,2*], Behdad Pouran[1,2], Harrie Weinans[1,2,3], Amir A. Zadpoor[1]

[1]*Department of Biomechanical Engineering, Faculty of Mechanical, Maritime, and Materials Engineering, Delft University of Technology, Mekelweg 2, 2628CD, Delft, The Netherlands*
[2]*Department of Orthopedics, UMC Utrecht, Heidelberglaan100, 3584CX Utrecht, The Netherlands*
[3]*Department of Rheumatology, UMC Utrecht, Heidelberglaan100, 3584CX Utrecht, The Netherlands*



**Abstract**

Analytical and numerical methods have been used to extract essential engineering parameters such as elastic modulus, Poisson's ratio, permeability and diffusion coefficient from experimental data in various types of biological tissues. The major limitation associated with analytical techniques is that they are often only applicable to problems with simplified assumptions. Numerical multi-physics methods, on the other hand, enable minimizing the simplified assumptions but require substantial computational expertise, which is not always available. In this paper, we propose a novel approach that combines inverse and forward artificial neural networks (ANNs) which enables fast and accurate estimation of the diffusion coefficient of cartilage without any need for computational modeling. In this approach, an inverse ANN is trained using our multi-zone biphasic-solute finite-bath computational model of diffusion in cartilage to estimate the diffusion coefficient of the various zones of cartilage given the concentration-time curves. Robust estimation of the diffusion coefficients, however, requires introducing certain levels of stochastic variations during the training

[*]Corresponding author, e-mail addresses: v.arbabi@gmail.com &v.arbabi@tudelft.nl, Tel.: +31-15-2784239, Fax: +31-15-2784717.

process. Determining the required level of stochastic variation is performed by coupling the inverse ANN with a forward ANN that receives the diffusion coefficient as input and returns the concentration-time curve as output. Combined together, forward-inverse ANNs enable computationally inexperienced users to obtain accurate and fast estimation of the diffusion coefficients of cartilage zones. The diffusion coefficients estimated using the proposed approach are compared with those determined using direct scanning of the parameter space as the optimization approach. It has been shown that both approaches yield comparable results.

**Keywords**: artificial neural network, diffusion coefficient, biphasic-solute finite element, micro-computed tomography, finite bath, noise cancellation



## 1. INTRODUCTION

Transport of molecules in articular cartilage depends on factors such as orientation and concentration of collagen fibrils, proteoglycans, and water content, which vary significantly across cartilage thickness (Leddy and Guilak, 2008). The rate of transport can be affected by the progression of the most common disease of diarthrodial joints, i.e. osteoarthritis (OA), which is due to changes in molecular structure of cartilage (Arbabi et al., 2015b; Huttunen et al., 2014; Ko and Quinn, 2013; Kokkonen et al., 2011a; Pouran et al., 2015). Molecular transport (diffusion) plays a key role in monitoring OA progression, delivery of therapeutics and nutrients as well as in the exchange of signaling molecules between cartilage and its surrounding tissues of subchondral bone and synovial fluid (Jackson and Gu, 2009; Pan et al., 2012; Pan et al., 2009). Previous studies used analytical solutions, mathematical fits, and computational models to derive the diffusion coefficients of solutes in cartilage (Arbabi et al., 2015b; Ateshian et al., 2011; Ateshian et al., 2012; Huttunen et al., 2014; Kokkonen et al., 2011a; Kokkonen et al., 2011b). The available analytical solutions can only be applied to problems where either simple geometries are used or simplified assumptions are made

(Crank, 1979). Occasionally mathematical fits have been used when analytical solutions were not available, however, since mathematical formulae involving diffusion coefficients are fitted to the experimental data, the physical importance of certain phenomena might be neglected (Kokkonen et al., 2011a). Computational models have been used to obtain the diffusion coefficient of neutral and charged solutes in complex geometries (Arbabi et al., 2015b; Ateshian et al., 2011). Nevertheless, computational models are often associated with optimization algorithms which require advanced computational expertise while being cumbersome and lacking the capacity to recognize pattern of the experimental data.

Artificial neural networks (ANNs) are considered as intelligent tools which can be trained using input data and output target to efficiently fulfill pattern recognition (Arbabi et al., 2015a). In biomechanics, ANNs have been applied to problems such as bone remodeling, indentation tests as well as sport/gait mechanics (Campoli et al., 2012; Darling and Guilak, 2008; Hahn et al., 2005; Oh et al., 2013; Zadpoor et al., 2012).

Previously, we described a finite-bath finite element model and derived the diffusion coefficients of a neutral solute across cartilage zones using direct scanning of the parameter space as the optimization algorithm (Arbabi et al., 2015b). We aim to create a package that can obtain the diffusion coefficients of a neutral solute in cartilage zones using series of micro-computed tomography (micro-CT) data even in labs where no computational expertise is available. From our previous studies, we know that ANNs are extremely sensitive to deviations from their underlying model (Arbabi et al., 2015a). To improve the robustness of ANN the training data has to be contaminated with some level of stochastic variation i.e. noise. Since the required level of noise is generally unknown, we have proposed, for the first time, to use a second ANN that could be used to estimate the required level of noise. The combination of both ANNs (after training) enables estimating the diffusion coefficients of a neutral solute across different zones of cartilage without any computational modeling.

## 2. METHODOLOGY

### *2.1. Experiments*

The descriptive details of the experiments consisting of sample preparation, image acquisition, and image processing are presented elsewhere (Arbabi et al., 2015b; Pouran et al., 2015). Osteochondral plugs ($n$=3, cartilage thickness= 2.8 mm, and diameter= 8.5 mm) were extracted from two fresh equine femora using custom-made drill bits while the site of extraction was constantly sprayed using phosphate buffer solution (PBS) to prevent overheating. Iodixanol solutions (finite bath of 650 µL, 1550.2 g/mol, charge=0, condition A: 420 mM, 290 mOsm/kg $H_2O$, condition B: 420 mM, 600 mOsm/kg $H_2O$, condition C: 210 mM, 290 mOsm/kg $H_2O$, GE Healthcare, The Netherlands) were prepared and the diffusion of Iodixonal from each condition was restricted to occur only from the articular surface of cartilage (Figure 1a). A micro-CT scanner (40 µm spatial resolution, Quantum FX, Perkin Elmer, USA) allowed monitoring the transport of Iodixonal through cartilage at room temperature. After each experiment, samples underwent desorption process using a large bath of PBS and protease inhibitor (*cOmplete*, Roche, The Netherlands). Using the in-built software of micro-CT (Analyze 11.0), 2D slices with TIFF format were generated. The mid-sagittal slice was then isolated and processed to render the concentration-time curves for 17 different time points until 48 hours (Figure 2).

### *2.2 Computational model*

The required equations to describe the transport of iodixanol across cartilage are conservation of linear momentum for the mixture, conservation of the mass for the mixture, and conservation of mass for solute, which were described in our previous work (Arbabi et al., 2015b). We assigned a neo-Hookean material model for cartilage with a Young's modulus of 10 MPa, Poisson's ratio of 0, hydraulic permeability of $10^{-3}$ $mm^4/Ns$, and effective solubility of 1. Diffusion coefficient of iodixanol was set to 0.00025 $mm^2/s$ (Nair et al., 2008) and the

diffusion tensor was assumed isotropic. Since cartilage is a heterogeneous material, we used a previously proposed multi-zone model where water content varied from 0.8 in the superficial zone (20% of the cartilage thickness) to 0.7 in the middle zone (50% of the cartilage thickness) and 0.6 in the deep zone (30% of the cartilage thickness) (Sophia Fox et al., 2009)(Figure 1b). The required initial and boundary conditions to solve the problem have been presented earlier (Arbabi et al., 2015b).

*2.3 Inverse-forward artificial neural networks*

A conventional feed-forward ANN consists of artificial neurons that is trained using a set of input data and a set of target data. The trained ANN processes the data in the hidden layer and generates the result as the output signal (Figure 3). Each artificial neuron in the hidden layer has a so-called signal activation function such as tang-sigmoid function which processes the signal transmitted by the other artificial neurons, gives a weight to it, and biases it to generate the output signal (Arbabi et al., 2015a). The biphasic-solute multi-zone finite element modeling was performed in FEBio for a wide range of diffusion coefficients in the superficial (0.1-99.1 $\mu m^2/s$ with interval 1 $\mu m^2/s$) and middle zones (0.1-10 $\mu m^2/s$ with interval 0.1 $\mu m^2/s$) resulting in 10,000 models, based on the findings of our previous study (Arbabi et al., 2015b). Using a FEBio-MATLAB interfacing program developed in-house, concentration-time curves (10,000×17 time points) were obtained from the biphasic-solute multi-zone finite element model and constituted the input matrix of the so-called inverse ANN while diffusion coefficients of superficial and middle zones (10,000×2 diffusion coefficients) served as the target matrix of the same ANN. Since the diffusion within the deep zone is not high enough to enable accurate determination of diffusion coefficient in the deep zone, we did not report the diffusion coefficients of the deep cartilage zone (Arbabi et al., 2015b). Our previous study showed that ANNs are very sensitive to any deviations from the underlying computational model that is used for their training (Arbabi et al., 2015a). To

alleviate this problem, the training data of ANNs can be contaminated with some level of noise (Arbabi et al., 2015a; Derks et al., 1997; Zur et al., 2009) to increase the robustness of ANN. Therefore, we trained the ANN using the input concentration vs. time curves contaminated with different levels of Gaussian noise, i.e. 1-20%. The contaminated concentration function ( $c'(t)$ ) is produced as follows:

$$c'(t) = c(t) + N(0, \sigma(t)) \tag{1}$$

where $N(0, \sigma(t))$ is a Gaussian distribution function with the standard deviation $\sigma(t) = c(t)/\lambda$ , and $c(t)$ is the concentration data obtained from finite element modeling. The parameter $\lambda$ represents the signal to noise ratio, which varies between 100 and 5 with step-size of 5 corresponding to noise levels 1-20%. We used 90% of the input data for the training, 5% for the validation, and 5% for the test of the ANN (30 neurons in the hidden layer).

Next, we introduce the experimental concentration vs. time curves to the trained inverse ANNs to obtain diffusion coefficients of superficial ($D_{Superficial}$) and middle ($D_{Middle}$) zones corresponding to each noise level as the outputs. The only remaining question to answer is 'what level of noise should be used for contaminating the training data of the inverse ANN?' This question cannot be answered in the general case without performing the actual finite element simulation to see which noise level produces diffusion coefficients that result in concentration-time curves that are as close as possible to the experimental values of the concentration-time curve. To circumvent this problem and avoid performing direct finite element simulations, we propose a novel approach that is based on using a forward ANN. This second ANN receives the diffusion coefficients as input and returns the concentration-time curve associated with those values of diffusion coefficients. To maximize the fidelity of the forward ANN to the actual finite element simulations, fully clean training data is used for its training. Similar to inverse ANN, we used 90% of the input data for training, 5% for validation, and 5% for testing the forward ANN (30 neurons in the hidden layer). The

diffusion coefficients estimated by the inverse ANN were then fed back to the forward ANN to estimate the concentration-time curve. The noise level was optimized to minimize the root mean square error (RMSE) between the experimental concentration-time curve and the concentration-time curve estimated by the forward ANN (Figure 4). A MATLAB code for generating noisy data and training inverse-forward artificial networks is available in the Appendix.

## 3. RESULTS

The high values of the Pearson correlation coefficients (R) clearly showed robustness of the inverse ANN when trained under different levels of noise (e.g. Figure 5a-c). The mean squared error drops to very low values for the training, validation, and test datasets, thereby confirming the efficacy of the training process (Figure 5d). All training, validation, and test datasets showed similar improvement as the training iterations progressed (Figure 5d). The identification error, i.e. the difference between the actual set of diffusion coefficients and those predicted by inverse ANN, for the test dataset that was not used in training process, was reminiscence of a normal distribution and was quite small (e.g. Figure 5e). Similar results were obtained for all levels of noise and the same observations held true (data not shown).

The Pearson correlation coefficients for the forward ANN for all training, validation, and test datasets was equal to one (Figure 6a-c), which suggests perfect capability of the forward ANN in replacing the actual finite element model for the purpose of predicting the concentration-time curve given the diffusion coefficient. Similar to inverse ANN, the training diagram of the inverse ANN reveals a very small mean squared error for the training, validation, and test datasets, which further confirms the efficacy of the training process (Figure 6d).

The combined forward-inverse ANN approach proposed here and the direct scanning of the parameter space as the optimization approach resulted in similar values of diffusion

coefficients (Table 1b) and similar concentration-time curves for all the cartilage samples for which experimental data were available from our previous experimental study (Figure 2). The coefficient of determination ($R^2$) and RMSE between were similar for the combined forward-inverse ANN approach and the optimization approach (Table 1a). Except for sample 3 and condition C where the required noise level in the training phase was around 7%, the other samples and conditions resulted in required noise levels below 2.5% (Table 1b).

## 4. DISCUSSION

Interpretation of experimental data in tissue biomechanics often requires the use of complex material models such as multiphasic, biphasic-solute, as well as complex boundary conditions and/or geometries. Analytical and computational solutions have been developed to interpret experimental data while capturing the real multi-physics phenomena to the maximum possible extent (Arbabi et al., 2015b, 2016; Ateshian et al., 2011; Ateshian et al., 2012). Computational models such as FEM can remarkably boost the solution for more complex problems when complicated material models, boundary conditions, and geometries are concerned (Ateshian et al., 2013). The major drawback of computational models is that they are time-consuming to develop and require considerable computational modeling and mathematical physics expertise.

Recently, we developed a multi-zone multi-physics model to study the transport of neutral solutes across articular cartilage which enabled us estimate the diffusion coefficients of different cartilage layers (Arbabi et al., 2015b). In spite of being a powerful approach for accurate estimation of diffusion coefficients, computational models similar to the one proposed in our previous study require considerable computational expertise that is not universally available. Based on the proposed method regarding the trained ANNs with noise (Arbabi et al., 2015a) in the present study we aimed to obtain the diffusion coefficients of different cartilage layers using experimental data collected during diffusion experiments. In

the current work we proposed to combines inverse and forward artificial neural networks (ANNs) to provide a fast and accurate estimation of the diffusion coefficient of cartilage without any need for computational modeling to simulate the diffusion. Determining the required level of stochastic variation was performed by coupling the inverse ANN with the forward ANN, which receives the concentration-time curve and returns the diffusion coefficient.

This approach presented in this study is not only capable of cancelling the noise, but also eliminates the need for FEM knowledge. The first element of the inverse-forward ANNs is the inverse ANN which is trained with noisy data and is responsible to filter the noise, while the second element is the forward ANN which eliminates the necessity of FEM. Training with noise-free FEM data of the inverse ANN would result in overfitting and its subsequent failure (Arbabi et al., 2015a; Zur et al., 2009). The inverse ANN trained with noisy data (Gaussian random noise) is most sensitive to the general trend of the experimental data without being influenced by small deviations from FEM caused by uncertainties involved in the experimental data.

The pattern recognition feature of ANN has been previously stressed and our findings also underscored this feature (Arbabi et al., 2015a; C. M. Bishop, 1995). The difference between RMSE and $R^2$ from optimization algorithm and ANN predictions although not large (Table 1a), might be due to differences in interval step sizes by which ANN was trained and optimization algorithm was processed.

By training the ANN using sufficiently wide range of diffusion coefficients for different thicknesses of cartilage, different bath sizes and concentrations, non-FEM specialists can easily benefit from the application of the inverse-forward ANNs proposed in this work. Besides, since ANN has been shown to be applicable for both indentation of poroelastic materials (Arbabi et al., 2015a) and our diffusion experiments, one can take advantage of it in

other areas of tissue biomechanics where complex multi-physics computational models are needed to estimate specific properties of tissues.

More complex computational models particularly nonlinear (i.e. hyperplastic) models may be needed for estimation of the diffusion coefficients of cartilage under different (loading) conditions. For example, there is some evidence that loading may influence the process of solute transport in cartilage (Entezari et al., 2014; Mauck et al., 2003). Experiments that investigate the effect of mechanical loading on the diffusion process may therefore be associated with relatively high levels of strain in cartilage, thereby necessitating the use of hyperplastic models for describing the elastic part of the cartilage mechanical behavior. The presence of large deformations and the use of hyperplastic models introduce strong nonlinearities in the involved equations one of the consequences of which may be non-uniqueness of the solutions to the problem of identifying the physical properties of cartilage. It is important to assess the capability of ANN in estimating the diffusion coefficient in the cases where, similar to the case of large deformations, strong nonlinearity is present. Handling non-uniqueness is one of the challenging tasks for ANNs because non-uniqueness in the training data may confuse the training process of ANN and make it difficult for the ANN to find even one of the (non-unique) solutions of the problem.

The present study has several limitations. First, cartilage was modeled as a laterally isotropic material, although it is intrinsically an anisotropic material mainly due to spatial differences in terms of collagen fiber distribution/orientation. The molecular size has been shown to influence the diffusion, however, its effect could not be considered by the software used in this study. These limitations are, however, the intrinsic limitations of the full computational model which is used for training the forward and inverse ANNs. Should these limitations be remedied in the full computational model, it is expected that their correction can be reflected

in the proposed approach simply by using training data that are generated using the improved finite element model.

In summary, a novel algorithm combining inverse and forward ANNs was proposed to estimate the diffusion coefficient of the various zones of cartilage based on multi-physics model. The diffusion coefficients obtained using the proposed approach were found to be similar to the ones obtained using the conventional approach of combining full multi-physics computational models and optimization algorithms. This approach, however, has an important advantage as compared to the conventional approaches: researchers and labs without computational modeling expertise can use it effortlessly, although it should be noted that the methodology of this work urges for initial FEM expertise but once established for a specific tissue type e.g. equine cartilage with similar morphology, no further computational skill will be required. The proposed algorithm comprising of inverse-forward ANNs which could cancel out the input data noise (inverse-ANN) and eliminate the need for FEM expertise (forward-ANN) as much as possible could be used for similar biomechanical applications.

**Conflict of Interest**

The authors of this work do not enclose any conflict of interests.

## REFERENCES

Arbabi, V., Pouran, B., Campoli, G., Weinans, H., Zadpoor, A.A., 2016a. Determination of the mechanical and physical properties of cartilage by coupling poroelastic-based finite element models of indentation with artificial neural networks. Journal of biomechanics 49, 631-637.

Arbabi, V., Pouran, B., Weinans, H., Zadpoor, A.A., 2015b. Transport of Neutral Solute Across Articular Cartilage: The Role of Zonal Diffusivities. Journal of biomechanical engineering 137, 071001-071001.

Arbabi, V., Pouran, B., Weinans, H., Zadpoor, A.A., 2016. Multiphasic modeling of charged solute transport across articular cartilage: Application of multi-zone finite-bath model. Journal of biomechanics 49, 1510-1517.

Ateshian, G.A., Albro, M.B., Maas, S., Weiss, J.A., 2011. Finite element implementation of mechanochemical phenomena in neutral deformable porous media under finite deformation. Journal of biomechanical engineering 133, 081005.

Ateshian, G.A., Maas, S., Weiss, J.A., 2012. Solute transport across a contact interface in deformable porous media. Journal of biomechanics 45, 1023-1027.

Ateshian, G.A., Maas, S., Weiss, J.A., 2013. Multiphasic Finite Element Framework for Modeling Hydrated Mixtures With Multiple Neutral and Charged Solutes. Journal of biomechanical engineering 135, 111001-111001.

C. M. Bishop, 1995. Neural Networks for Pattern Recognition. Oxford University Press, New York.

Campoli, G., Weinans, H., Zadpoor, A.A., 2012. Computational load estimation of the femur. Journal of the mechanical behavior of biomedical materials 10, 108-119.

Crank, J., 1979. The mathematics of diffusion. Clarendon Press:, Oxford, Eng:.

Darling, E.M., Guilak, F., 2008. A neural network model for cell classification based on single-cell biomechanical properties. Tissue engineering. Part A 14, 1507-1515.

Derks, E.P.P.A., Pauly, B.A., Jonkers, J., Timmermans, E.A.H., Buydens, L.M.C., 1997. Adaptive noise cancellation on inductively coupled plasma spectroscopy. Chemometrics and Intelligent Laboratory Systems 39, 143-159.

Entezari, V., Bansal, P.N., Stewart, R.C., Lakin, B.A., Grinstaff, M.W., Snyder, B.D., 2014. Effect of mechanical convection on the partitioning of an anionic iodinated contrast agent in intact patellar cartilage. Journal of orthopaedic research : official publication of the Orthopaedic Research Society 32, 1333-1340.

Hahn, M.E., Farley, A.M., Lin, V., Chou, L.-S., 2005. Neural network estimation of balance control during locomotion. Journal of biomechanics 38, 717-724.

Huttunen, J.M.J., Kokkonen, H.T., Jurvelin, J.S., Töyräs, J., Kaipio, J.P., 2014. Estimation of fixed charge density and diffusivity profiles in cartilage using contrast enhanced computer tomography. International Journal for Numerical Methods in Engineering 98, 371-390.

Jackson, A., Gu, W., 2009. Transport Properties of Cartilaginous Tissues. Current rheumatology reviews 5, 40.

Ko, Lok S., Quinn, Thomas M., 2013. Matrix Fixed Charge Density Modulates Exudate Concentration during Cartilage Compression. Biophysical journal 104, 943-950.

Kokkonen, H.T., Jurvelin, J.S., Tiitu, V., Toyras, J., 2011a. Detection of mechanical injury of articular cartilage using contrast enhanced computed tomography. Osteoarthritis and cartilage / OARS, Osteoarthritis Research Society 19, 295-301.

Kokkonen, H.T., Mäkelä, J., Kulmala, K.A.M., Rieppo, L., Jurvelin, J.S., Tiitu, V., Karjalainen, H.M., Korhonen, R.K., Kovanen, V., Töyräs, J., 2011b. Computed tomography detects changes in contrast agent diffusion after collagen cross-linking typical to natural aging of articular cartilage. Osteoarthritis and Cartilage 19, 1190-1198.

Leddy, H.A., Guilak, F., 2008. Site-specific effects of compression on macromolecular diffusion in articular cartilage. Biophysical journal 95, 4890-4895.

Mauck, R.L., Hung, C.T., Ateshian, G.A., 2003. Modeling of Neutral Solute Transport in a Dynamically Loaded Porous Permeable Gel: Implications for Articular Cartilage Biosynthesis and Tissue Engineering. Journal of biomechanical engineering 125, 602-614.

Nair, N., Kim, W.J., Braatz, R.D., Strano, M.S., 2008. Dynamics of surfactant-suspended single-walled carbon nanotubes in a centrifugal field. Langmuir : the ACS journal of surfaces and colloids 24, 1790-1795.

Oh, S.E., Choi, A., Mun, J.H., 2013. Prediction of ground reaction forces during gait based on kinematics and a neural network model. Journal of biomechanics 46, 2372-2380.

Pan, J., Wang, B., Li, W., Zhou, X., Scherr, T., Yang, Y., Price, C., Wang, L., 2012. Elevated cross-talk between subchondral bone and cartilage in osteoarthritic joints. Bone 51, 212-217.

Pan, J., Zhou, X., Li, W., Novotny, J.E., Doty, S.B., Wang, L., 2009. In situ measurement of transport between subchondral bone and articular cartilage. Journal of orthopaedic research : official publication of the Orthopaedic Research Society 27, 1347-1352.

Pouran, B., Arbabi, V., Zadpoor, A.A., Weinans, H., 2016. Isolated effects of external bath osmolality, solute concentration, and electrical charge on solute transport across articular cartilage. (under review).

Sophia Fox, A.J., Bedi, A., Rodeo, S.A., 2009. The Basic Science of Articular Cartilage: Structure, Composition, and Function. Sports Health 1, 461-468.

Zadpoor, A.A., Campoli, G., Weinans, H., 2012. Neural network prediction of load from the morphology of trabecular bone. Applied Mathematical Modelling 37, 5260-5276.

Zur, R.M., Jiang, Y., Pesce, L.L., Drukker, K., 2009. Noise injection for training artificial neural networks: a comparison with weight decay and early stopping. Med Phys 36, 4810-4818.

**Figure captions**

**Figure 1.** Experimental (a) versus computational (b) models: Iodixonal finite bath is placed on the surface of the articular cartilage to study its axial diffusion across various zones of articular cartilage i.e. superficial zone (20% of cartilage thickness), middle zone (50% of cartilage thickness) and deep zone (30% of cartilage thickness)

**Figure 2.** Normalized concentration of Iodixonal versus time for samples 1-3 and conditions A-C: points represent the experimental data, solid line is the inverse-forward ANNs result and dashed line is the optimization algorithm result

**Figure 3.** Anatomy of the inverse-forward ANNs

**Figure 4.** Flowchart of inverse-forward ANNs to obtain diffusion coefficients

**Figure 5.** Regression diagrams for the training (a), validation (b), and test (c) datasets of the inverse ANN trained when it was trained with signal to noise ratio of 50 (2% noise level). ANN training diagram (d) and histogram of identification errors (e).

**Figure 6.** Regression diagrams for the training (a), validation (b), and test (c) datasets of the forward-ANN (noise-free). ANN training diagram (d).



**Table captions**

**Table 1.** $R^2$ and RMSE for samples 1-3 and conditions A-C for inverse-forward ANNs and optimization algorithm (a), Diffusion coefficients in the superficial ($D_{Superficial}$) and middle ($D_{Middle}$) zones obtained using inverse-forward ANNs and optimization algorithm (b).

**Table 1**

**(a)**

| | Condition | A | | B | | C | |
|---|---|---|---|---|---|---|---|
| | | ANN | Optimization | ANN | Optimization | ANN | Optimization |
| Sample 1 | $R^2$ | 1.00 | 0.99 | 1.00 | 1.00 | 0.99 | 0.99 |
| | RMSE | 0.0059 | 0.0068 | 0.0052 | 0.0044 | 0.0131 | 0.0122 |
| Sample 2 | $R^2$ | 0.99 | 1.00 | 0.99 | 0.99 | 0.99 | 0.99 |
| | RMSE | 0.0081 | 0.0058 | 0.0068 | 0.0074 | 0.01 | 0.0079 |
| Sample 3 | $R^2$ | 0.97 | 0.97 | 0.95 | 0.95 | 0.95 | 0.94 |
| | RMSE | 0.0230 | 0.0207 | 0.0330 | 0.0348 | 0.0320 | 0.0349 |

**(b)**

| | | Diffusion coefficient ($\mu m^2/s$) | | | | | |
|---|---|---|---|---|---|---|---|
| | Condition | A | | B | | C | |
| | | $D_{Superficial}$ | $D_{Middle}$ | $D_{Superficial}$ | $D_{Middle}$ | $D_{Superficial}$ | $D_{Middle}$ |
| Sample 1 | ANN | 8.00 | 0.48 | 5.28 | 0.35 | 11.5 | 1.20 |
| | Optimization | 7.50 | 0.55 | 5.30 | 0.30 | 13.00 | 1.00 |
| Sample 2 | ANN | 9.34 | 0.59 | 8.00 | 0.65 | 7.40 | 0.72 |
| | Optimization | 10.00 | 0.60 | 7.30 | 0.55 | 8.80 | 0.75 |
| Sample 3 | ANN | 26.00 | 1.85 | 35.20 | 3.50 | 60.40 | 3.50 |
| | Optimization | 30.00 | 2.25 | 35.00 | 3.00 | 60.00 | 4.00 |

**Figure 1**

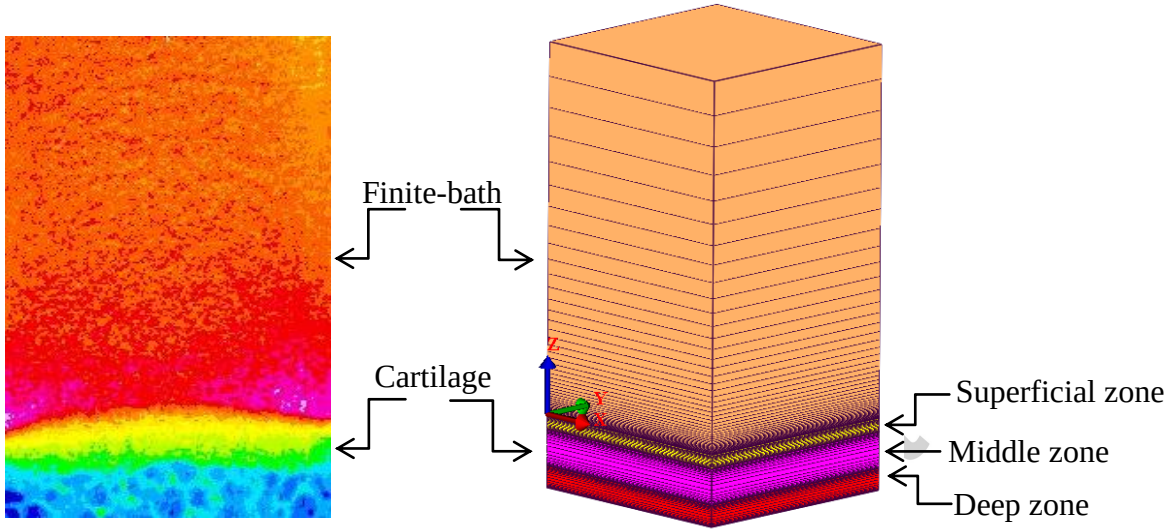

**Figure 2**

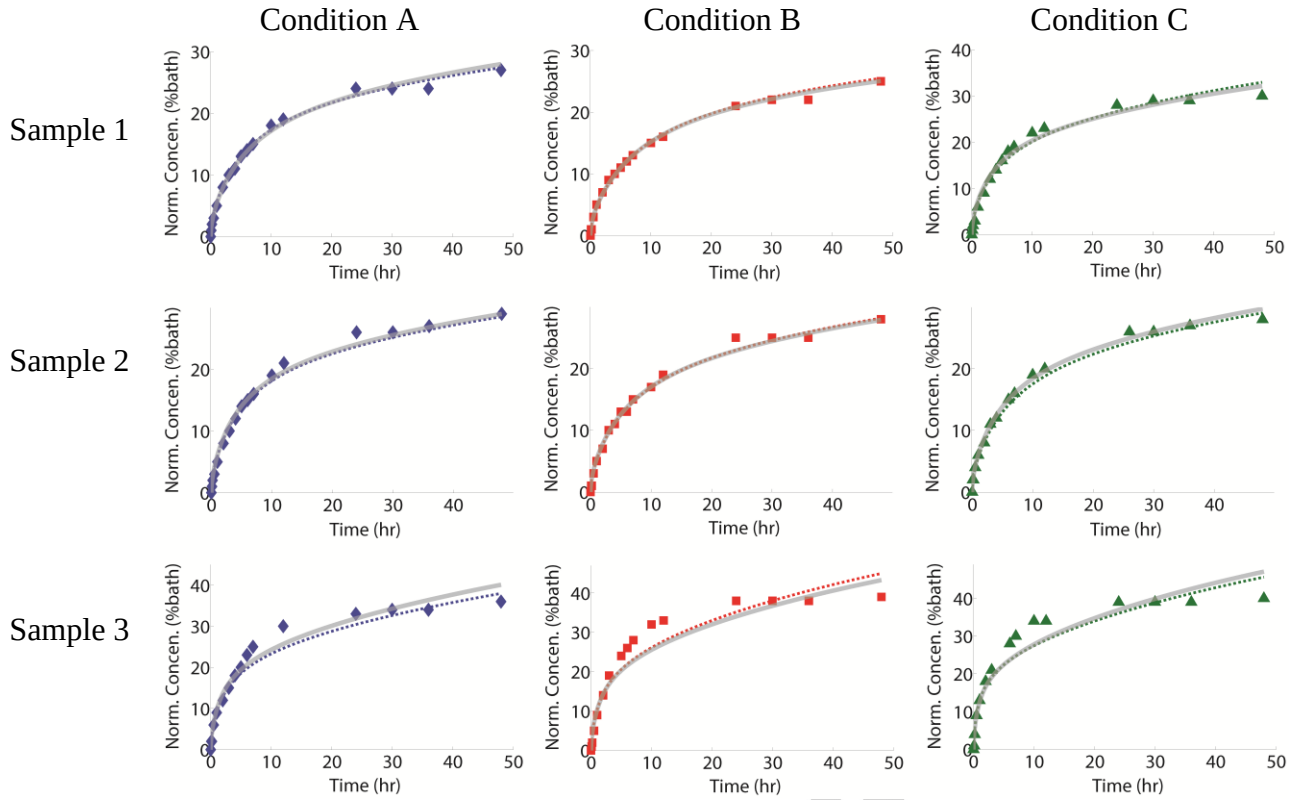

**Figure 3**

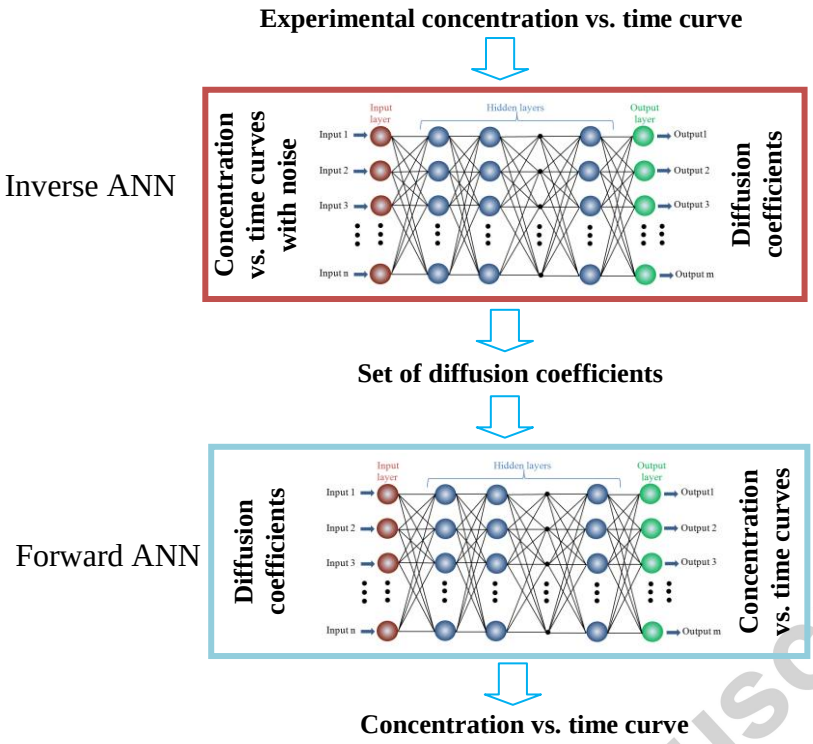

**Figure 4**

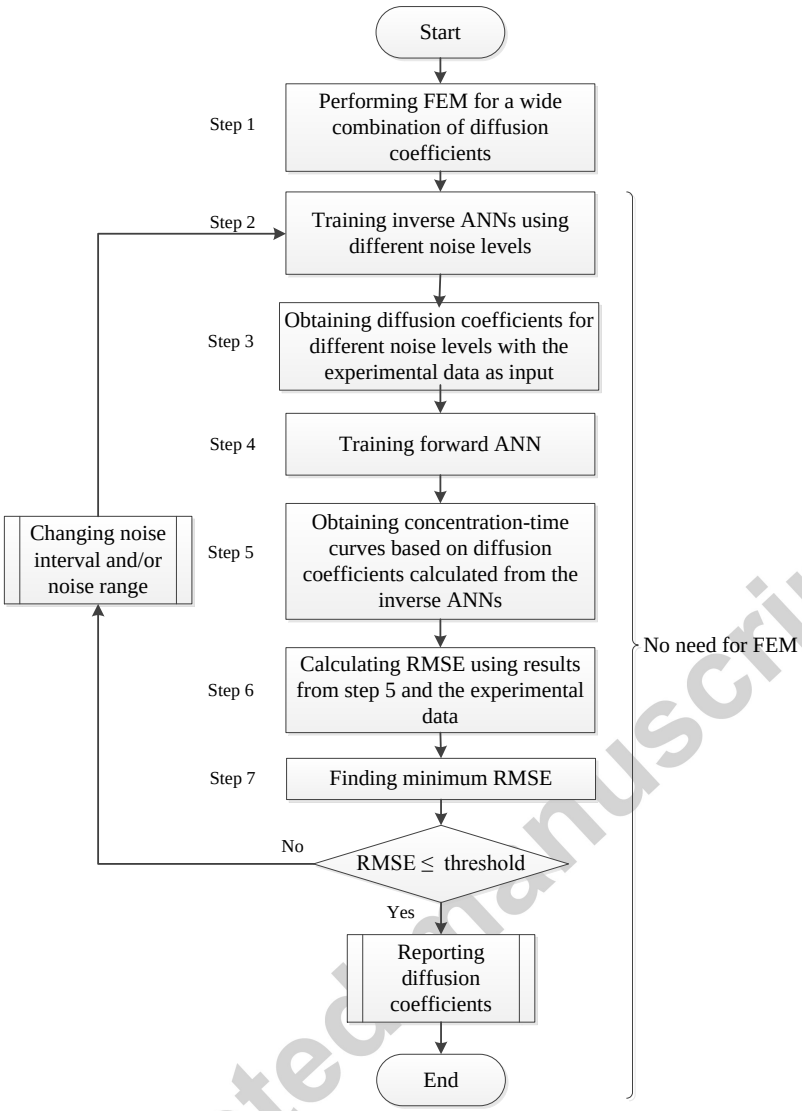

**Figure 5**

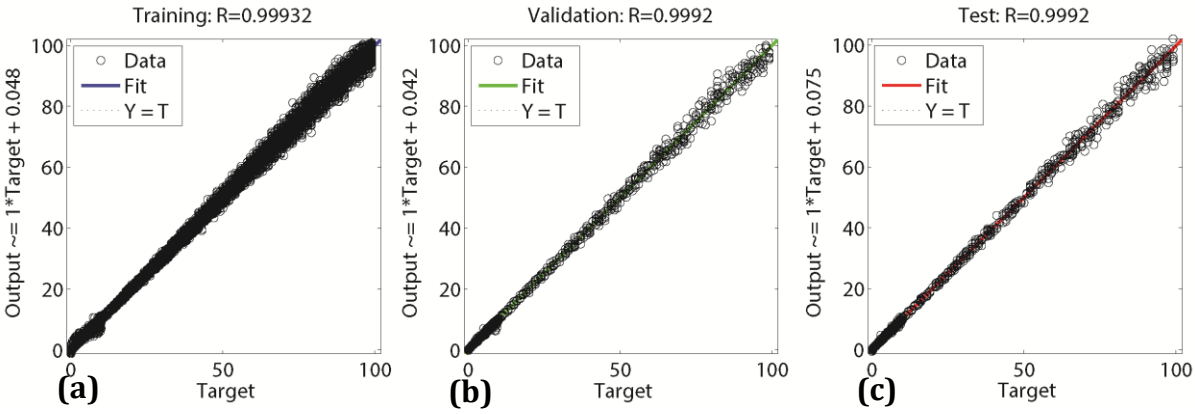


| No. samples | Training | Validation | Test | No. neurons |
|---|---|---|---|---|
| 10000 | 90% | 5% | 5% | 30 |

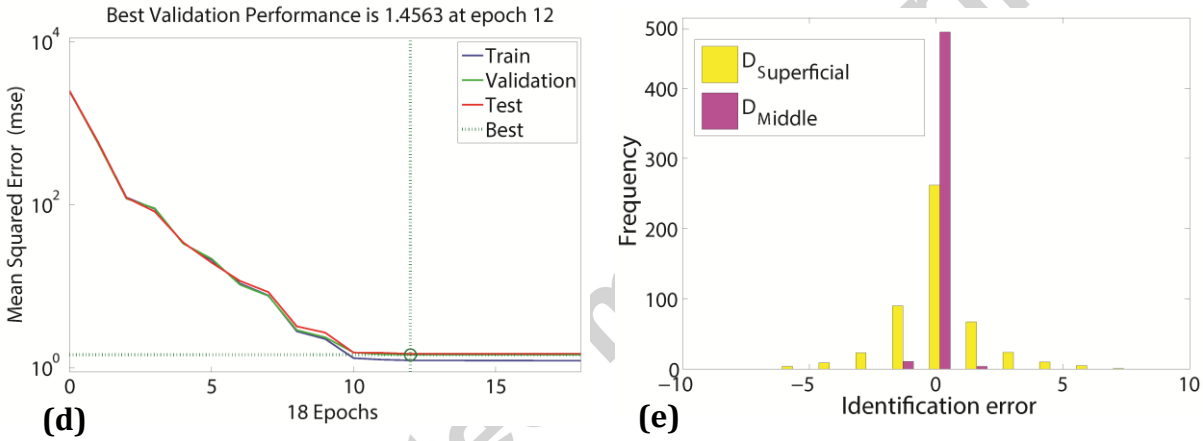

**Figure 6**

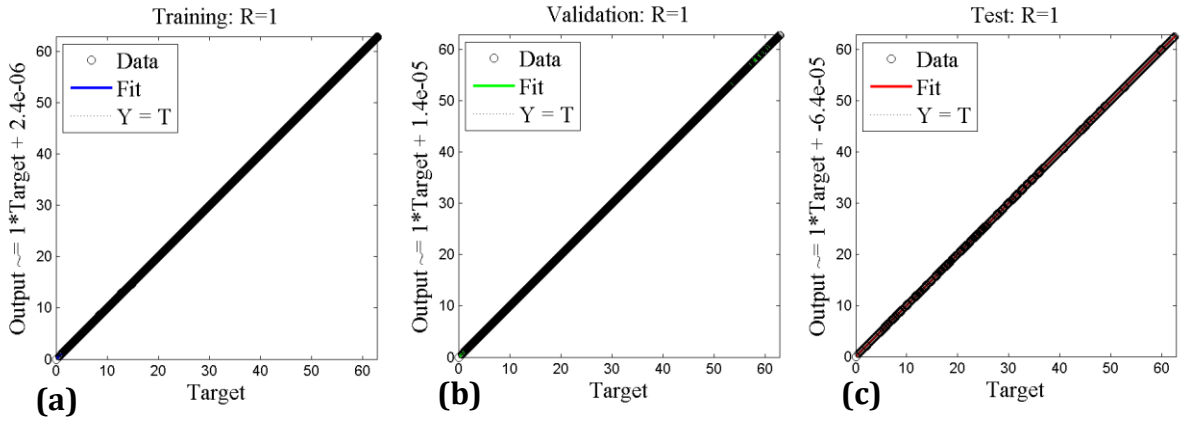


| No. samples | Training | Validation | Test | No. neurons |
|---|---|---|---|---|
| 10000 | 90% | 5% | 5% | 30 |